1 of 1

CONF-941144--126

EFFECT OF IRRADIATION SPECTRUM ON THE MICROSTRUCTURE OF ION-IRRADIATED Al_2O_3

S. J. ZINKLE
Metals and Ceramics Division, Oak Ridge National Laboratory, P.O. Box 2008, Oak Ridge, TN 37831-6376, USA.

ABSTRACT

Polycrystalline samples of alpha-alumina have been irradiated with various ions ranging from 3.6 MeV Fe^+ to 1 MeV H^+ ions at 650°C. Cross-section transmission electron microscopy was used to investigate the depth-dependent microstructure of the irradiated specimens. The microstructure following irradiation was observed to be dependent on the irradiation spectrum. In particular, defect cluster nucleation was effectively suppressed in specimens irradiated with light ions such as 1 MeV H^+ ions. On the other hand, light ion irradiation tended to accelerate the growth rate of dislocation loops. The microstructural observations are discussed in terms of ionization enhanced diffusion processes.

INTRODUCTION

Numerous radiation effects studies have been performed on alumina over the past 40 years (see refs. [1,2] for recent reviews). These studies have employed electron, light ion, heavy ion, or neutron irradiation sources, with the implicit assumption that the displacement damage produced by the different irradiation sources can be correlated via the modified Kinchin-Pease model [3] for displacement damage. It has been known for some time that the surviving defect fraction in metals is dependent on the mass of the bombarding particle (primary knock-on atom energy spectrum) [4,5]. It was recently shown by Agnew [6] that the efficiency of point defect production in alumina is also somewhat dependent on the mass of the bombarding ion.

Of even greater potential importance in irradiated ceramic insulators is the amount of ionization associated with the bombarding particles. Walker [7] demonstrated over 30 years ago that volumetric point defect swelling introduced in BeO by fission neutron irradiation could be annealed by subsequent exposure to 1 MeV electrons at 100°C. An extensive set of experiments on ion irradiated Al_2O_3 [8,9] and MgO [10] by Arnold and Krefft and coworkers clearly demonstrated that light ion irradiation produced less volumetric swelling (for a constant amount of displacement damage) compared to heavy ion irradiation. Furthermore, it was shown that the swelling induced by heavy ion irradiation could be recovered by exposure to either protons or 8 keV electrons. Since the electron energy of 8 keV was too low to produce displacement damage in alumina, these experiments gave a clear indication of the importance of ionizing radiation on radiation damage processes in ceramic insulators. Optical absorption measurements indicated that F centers (oxygen vacancy with 2 trapped electrons) were preferentially produced by heavy ion bombardment, whereas F^+ centers (oxygen vacancy with 1 trapped electron) were preferentially produced by light ion irradiation [10], and it was proposed that the recovery of swelling during light ion irradiation of heavy ion-implanted specimens was due to a change in the point defect charge state from F to F^+ [8-10]. A recent independent study has verified that 2 MeV He^+ ion irradiation of Xe^+ or Ca^+ ion implanted MgO produced annealing of the initial volumetric swelling, and that the He irradiation changed many of the F centers to F^+ centers [11]. It was also concluded that the He ion irradiation induced plastic flow which relieved some of the stress in the preimplanted region.

Unfortunately, electron microscopy was not used to investigate the microstructural changes associated with the light ion irradiations in these previous studies. Cross-section transmission electron microscopy (TEM) has recently been used to study the microstructural evolution in oxide ceramic insulators following irradiation with ions varying from 1 MeV H^+ to 3.6 MeV Fe^+ ions [12,13]. Recent results obtained on ion-irradiated alumina are summarized in this paper.

S. J. Zinkle

EXPERIMENTAL PROCEDURE

TEM disks of dimension 3 mm diam. by 0.5 mm thickness were cut from sintered bars of polycrystalline alpha-alumina (GE Lucalox or Wesgo AL995). The TEM disks were mechanically polished with 0.5 μm diamond paste to produce a smooth surface, and then irradiated at 650°C in the triple ion beam accelerator facility at ORNL. Specimens were irradiated with H, He, C, Al, or Fe ion beams at energies ranging from 1 MeV to 3.6 MeV with beam currents between 0.1 and 3 $\mu A/cm^2$. The ion beam fluxes and fluences were systematically varied on several of the target arrays in order to investigate the relative importance of damage rate and cumulative damage level. Further details of the irradiation conditions are given elsewhere [12,13]. The TRIM-90 computer code [14] was used to calculate the depth-dependent ionization and displacement damage dose. The measured [15] threshold displacement energies of 24 eV and 78 eV for the Al and O sublattices, respectively, were used in the TRIM calculations, and a sublattice-averaged displacement energy of 40 eV was used to convert the damage energies calculated by TRIM to displacements per atom (dpa). The calculated damage rates varied from ~10^{-6} to 10^{-3} dpa/s, with corresponding ionizing dose rates of 0.1 to 30 MGy/s, depending on ion species and flux.

Cross-section TEM specimens were prepared by gluing a mechanically polished nonirradiated specimen to the irradiated surface of each sample, sectioning perpendicular to the irradiation surface, mechanically dimpling, and ion milling in a liquid nitrogen-cooled stage (6 keV Ar ions, 15° sputtering angle) until perforation occurred at the glued interface [16]. The specimens were examined in a Philips CM12 electron microscope operating at 120 kV.

RESULTS

Figure 1 shows the microstructure of alumina following irradiation at 650°C with 3-MeV C^+ ions to a peak damage level of 0.5 dpa. A high density (~$5x10^{22}/m^3$) of small dislocation loops was observed to be uniformly distributed throughout the irradiation region. There was no significant variation in the loop size or density in the irradiated region, despite the depth-dependent variation in the damage level from ~0.03 dpa near the irradiated surface to ~0.5 dpa at the peak damage region (1.6 μm depth). Examination of specimens irradiated to higher damage levels and with different heavy ions such as 3.6-MeV Fe^+ and 2-MeV Al^+ indicated that the defect cluster size increased slightly with increasing dose (from ~5 nm at 0.02 dpa to ~15 nm at 20 dpa). In addition, the defect cluster density was nearly constant (0.5 to 1 x $10^{23}/m^3$) over this large range of damage levels. Irradiation at low fluence with different heavy ions indicated that the threshold dose for producing observable defect clusters in alumina at 650°C was ~0.005 dpa. There was no significant difference in the micro-structures of alumina specimens irradiated to a given damage level with heavy ions ranging from 3-MeV C^+ to 3.6-MeV Fe^+ ions.

Fig. 1. Cross-section weak-beam micrograph of alumina irradiated with 3-MeV C^+ ions to a fluence of $5x10^{19}$ C^+/m^2 (0.03 dpa at 0.5 μm).

The microstructure of alumina following irradiation at 650°C with 1-MeV H^+ or He^+ ions was noticeably different from the heavy ion results. The loop density in alumina irradiated with 1-MeV He^+ ions to a damage level of 0.5 dpa was about a factor of two lower than that measured in alumina irradiated to the same dose with 3 MeV C^+ or 2 MeV Al^+ ions. In addition, the average loop diameter at 0.5 dpa was

S. J. Zinkle
2
6

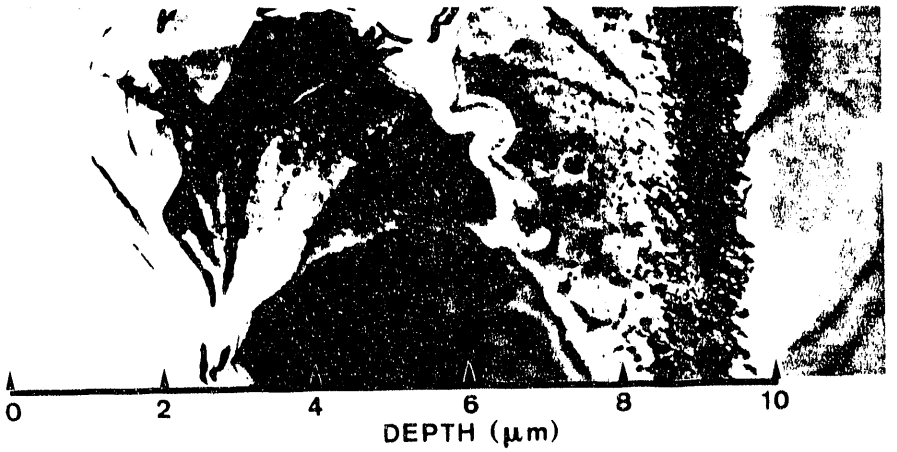

Fig. 2. Depth-dependent microstructure of alumina following irradiation at 650°C with 1-MeV H^+ ions to a fluence of 1.7×10^{22} H^+/m^2 (0.03 dpa at 0.5 μm).

about 50% larger than that observed in specimens irradiated with heavy ions. This trend towards a lower density of larger loops for the light ion irradiations was particularly pronounced in the case of 1-MeV protons. As shown in Fig. 2, dislocation loops were not observed outside of the implanted ion region (7 to 9.5 μm depth) in alumina irradiated at 650°C with 1-MeV H^+ ions at a flux of 6×10^{17} H^+/m^2-s. The dose in the defect-free irradiated regions (0 to 7 μm depth) ranged from 0.03 to ~0.5 dpa, which was well above the threshold dose for the formation of visible dislocation loops determined from the heavy ion irradiations of ~0.005 dpa.

A second set of specimens were irradiated at 650°C with 1-MeV protons at an order of magnitude lower flux (and fluence) than the specimen shown in Fig. 2 in order to investigate the effect of irradiation flux. A moderate density (~$3 \times 10^{20}/m^3$) of dislocation loops were visible at depths >0.8 μm from the irradiated surface for specimens irradiated to a fluence of 1.5×10^{21} H^+/m^2 (0.003 dpa at 1 μm) [12,13]. The average diameter of the loops for the low-flux specimens was ~35 nm, which is more than twice as large as the loop size for alumina specimens irradiated with heavy ions up to damage levels in excess of 20 dpa. This suggests that proton irradiation produces a suppression in loop nucleation and an enhancement in loop growth relative to heavy ion irradiation.

Figures 3 and 4 summarize the data on loop density and size, respectively, for the different bombarding ions. The arrow on the H^+ high flux datum in Fig. 3 denotes the upper limit for the loop density, since no loops were observed. The data are plotted as a function of the electronic- to nuclear-stopping power (ENSP) ratio. The ENSP ratio was calculated from TRIM-90 [14] at depths corresponding to the regions used for TEM analysis, which was midway between the surface and implanted ion regions. As discussed elsewhere [12,13], the ENSP ratio is an approximate measure of the amount of ionization produced in the lattice relative to the amount of displacement damage. Most of the energy lost by both light and heavy MeV ions is transferred to the electrons in the lattice, producing ionization. However, the relative amount of ionization (per displaced atom) is considerably higher for light ion irradiations compared to heavy ion irradiations. For example, the ENSP ratio is ~2000 for 1 MeV protons in alumina whereas it is only ~10 for 3.6-MeV Fe^+ ions. The corresponding ENSP ratios for alumina in a fusion (1st wall) and mixed-spectrum fission reactor are 13 and 100, respectively [13].

DISCUSSION

The TEM data summarized in Figs. 3 and 4 indicate that the loop size and density in irradiated alumina is rather insensitive to irradiation spectrum for heavy ion irradiations (ENSP ratio <1000), but is dramatically different for proton irradiation conditions (ENSP ratio ~2000). A similar dependence of the loop size and density on irradiation spectrum has been also observed for MgO

S. J. Zinkle

3

6

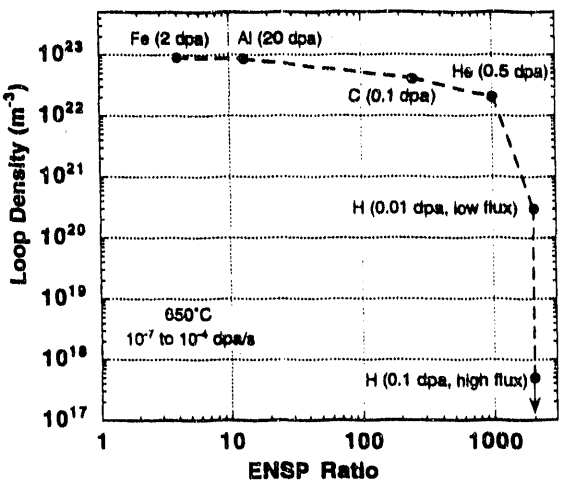

Fig. 3. Effect of ENSP ratio on the loop density in alumina irradiated with single ion beams at 650°C [13].

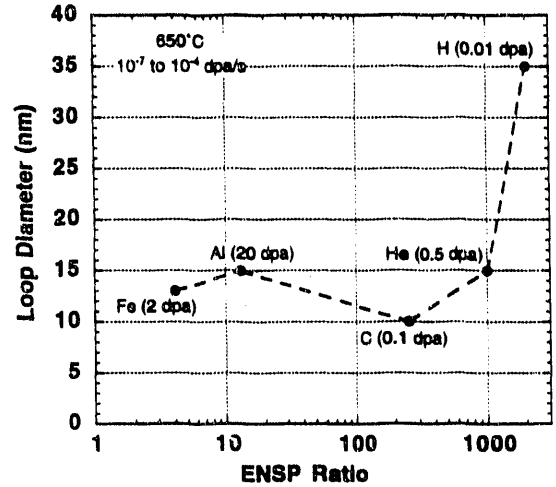

Fig. 4. Effect of ENSP ratio on the loop size in alumina irradiated with single ion beams at 650°C.

and magnesium aluminate spinel ($MgAl_2O_4$) [12,13]. The irradiation spectrum effect is particularly pronounced for spinel, where dislocation loop formation was not observed at 650°C for irradiation conditions which produced an ENSP ratio greater than ~20 [12,13]. It is worth noting that in all three oxide ceramics (MgO, Al_2O_3, and $MgAl_2O_4$) a rather sharp threshold exists between the high loop density (irradiation spectrum independent) regime and the low loop density regime. The threshold ENSP ratios for loop formation at 650°C for damage rates between 10^{-6} and 10^{-4} dpa/s are ~1000, ~500 and ~10 for Al_2O_3, MgO and $MgAl_2O_4$, respectively [12].

The increase in the dislocation loop size and decrease in loop density for the light ion irradiations are indicative of enhanced point defect diffusion. According to standard chemical rate theory calculations [17], enhanced point defect diffusion reduces the point defect supersaturation in the matrix and directly leads to a reduction in the nucleation rate of dislocation loops. Larger loop sizes are associated with the lower loop density since there are fewer loop nuclei competing for a given concentration of interstitials (loop nucleation is much more sensitive than loop growth to the point defect supersaturation). Defect-free regions were observed adjacent to grain boundaries in alumina irradiated with the low flux of 1-MeV protons (width ~0.5μm), and in spinel irradiated with several different light ions. The width of these defect-free regions adjacent to point defect sinks is proportional to $(D_iD_v/P)^{1/4}$ when point defect recombination is dominant, where D_i and D_v are the interstitial and vacancy diffusivities and P is the damage rate [18]. The D_iD_v product obtained from the proton irradiation defect-free zone width is many orders of magnitude larger than the value obtained from tracer diffusion (nonirradiation) studies [19]. Additional evidence for enhanced point defect diffusion in ceramics irradiated with light ions was obtained from room temperature irradiations of alumina and spinel [12,13]. For example, cavities with a mean diameter of 3 nm were observed to be aligned along the c-axis of alumina following a simultaneous triple beam (2 MeV Al, 1.4 MeV O and 0.2-0.4 MeV He ions) irradiation at room temperature to a damage level of 22 dpa [20]. The presence of nearly 1000 vacancies in each 3-nm diameter cavity is a clear indication of significant radiation-enhanced vacancy mobility in alumina during the room temperature irradiation, since vacancies would be expected to migrate less than one lattice jump distance during the 8 hour irradiation according to thermal diffusion data for alumina [19].

It is important to point out a significant difference between the radiation-enhanced diffusion commonly measured for irradiated metals and the present ionization-enhanced diffusion. The general expression for the atomic diffusion coefficient (ignoring mobile defect clusters) is given by

$$D = f_i D_i C_i + f_v D_v C_v \qquad (1)$$

S. J. Zinkle 4 6

where $f_{i,v}$ are geometric factors, $D_{i,v}$ are the interstitial and vacancy diffusivities, and $C_{i,v}$ are the interstitial and vacancy atomic concentrations [21]. The radiation enhanced diffusion observed in metals is due to supersaturations in the point defect concentrations ($C_{i,v}$) during irradiation, and is directly related to the displacement damage rate; radiation has no effect on the point defect diffusivities in metals. On the other hand, the enhancement in point defect diffusion observed in the present investigation was largest in regions where the damage rate was relatively low (e.g., in the near-surface and mid-range regions of the light ion-irradiated specimens) [12]. The dramatic decrease in the loop density in alumina when the proton irradiation flux was increased by a factor of 10 (Fig. 3) is also opposite to the behavior expected according to point defect supersaturation arguments (higher defect production rates should produce higher loop densities), and suggests that the accompanying ionizing radiation increases the interstitial diffusivity since loop nucleation depends on the product of D_iC_i. The apparent correlation of high point defect diffusion with large values of the E[illegible]P ratio (Figs. 3, 4) indicates that the enhanced diffusion in irradiated ceramics is associated wit[illegible] ionization effects which increase the point defect diffusivities ($D_{i,v}$). This conclusion is [illegible]o supported by the discrepancy between the irradiated and nonirradiated point defect diffusivi[illegible]s mentioned in the preceding paragraph.

It is well established that the point defect charge state can dramatically alter the migration energy of vacancies and interstitials in semiconductors and insulators [22-24]. It has also been shown experimentally that ionizing radiation produces a large enhancement in the diffusivity of vacancies [25] and hydrogen isotopes [26,27] in oxide insulators. As mentioned in the introduction, light ion irradiations preferentially produce a higher fraction of F^+ centers in oxide insulators, whereas heavy ions produce a larger proportion of F centers [10,11,28]. According to calculations, the diffusivity of F^+ centers is expected to be significantly higher than that of F centers in oxide insulators [24].

Further work is needed to verify that the anomalous microstructural evolution observed in oxide ceramics irradiated with light ions is solely due to ionization enhanced diffusion. For example, an ionization-enhanced increase in the point defect recombination volume could help the suppression of dislocation loop nucleation during light ion irradiation [13,29]. Due to the strong perturbation of the F^+ centers on surrounding lattice atoms [30], a higher rate of recombination of oxygen interstitials at F^+ centers would be expected compared to that at F centers. An additional factor that could be playing a role in the anomalous behavior of light ion-irradiated ceramics is the low average primary knockon atom (PKA) energy for light ion irradiations, which is not favorable for nucleating dislocation loops. As discussed elsewhere [12,13], however, the PKA spectrum does not seem to be the dominant factor responsible for the irradiation spectrum dependence. Regardless of the specific physical mechanism(s), it is apparent that proton and electron irradiations of ceramics are often not representative of fission or fusion neutron irradiation conditions. This finding is significant since ion and electron irradiations have often been used to develop the radiation effects data base of insulators that are intended for nuclear applications. For example, most of the data associated with the recently discovered phenomenon of radiation induced electrical degradation has been obtained from electron or light ion irradiations [31].

Only a limited set of experiments have been performed to date to examine the effect of variations in irradiation flux and temperature on the microstructural evolution in ion-irradiated alumina and spinel [12,13]. In qualitative terms, high fluxes appear to enhance point defect diffusion (as evidenced by a reduction in the loop density and an increase in the loop size), but further systematic experiments with several different ion beams at different irradiation temperatures are needed. Significant ionization-enhanced diffusion has been observed at both room temperature and 650°C, and the limited studies performed so far suggest that the point defect diffusion during light ion irradiation near room temperature is only slightly less than that at 650°C.

There is agreement between the present microstructural investigations [12,13] and previous physical property [7-11,28] and diffusion [25-28] studies that irradiation spectrum and flux effects are typically very significant in ceramic insulators. These irradiation spectrum and flux effects are much more pronounced in ceramics compared to metals, and need to be considered when comparing results obtained in different irradiation environments.

CONCLUSIONS

Alumina is relatively insensitive to changes in the irradiation spectrum associated with relatively heavy ions ranging from 3.6 MeV Fe^+ to 3 MeV C^+. Irradiation with 1 MeV protons produced a dramatic reduction in the dislocation loop density and an increase in the loop size compared to the heavy ion irradiations. Since even more pronounced effects have been observed in ion irradiated MgO and $MgAl_2O_4$, this indicates that proton and electron irradiations of ceramics are not representative of fission or fusion neutron irradiation conditions.

The most likely mechanism responsible for the irradiation spectrum dependence is ionization-enhanced point defect diffusion. Further work is needed to firmly establish the effect of irradiation flux and temperature. However, it is evident that irradiation spectrum (ionizing and displacive) and flux effects are much more pronounced in ceramics compared to metals. The ENSP ratio appears to be a useful parameter for evaluating irradiation spectrum effects in ceramics.

Acknowledgements

The ion irradiations were performed by S.W. Cook, and the TEM specimens were prepared by J.W. Jones and A.T. Fisher. This research was sponsored by the Office of Fusion Energy, US Department of Energy, under contract DE-AC05-84OR21400 with Martin Marietta Energy Systems, Inc.

REFERENCES

1. G.P. Pells, J. Amer. Cer. Soc. **77**, 368 (1994).
2. G.P. Pells, in *Microstructure of Irradiated Materials*, edited by I.M. Robertson et al. (Mater. Res. Soc., Pittsburgh, PA, 1995) these proceedings.
3. M.J. Norgett, M.T. Robinson and I.M. Torrens, Nucl. Eng. Des. **33**, 50 (1975).
4. R.S. Averback, R. Benedek and K.L. Merkle, Phys. Rev. B **18**, 4156 (1978).
5. S.J. Zinkle and B.N. Singh, J. Nucl. Mater. **199**, 173 (1993).
6. P. Agnew, Nucl. Instr. Meth. B **65**, 305 (1992).
7. D.G. Walker, J. Nucl. Mater. **14**, 195 (1964).
8. G.W. Arnold, G.B. Krefft and C.B. Norris, Appl. Phys. Lett. **25**, 540 (1974).
9. G.B. Krefft and E.P. EerNisse, J. Appl. Phys. **49**, 2725 (1978).
10. G.B. Krefft, J. Vac. Sci. Technol. **14**, 533 (1977).
11. R. Brenier, et al., Nucl. Instr. Meth. B **80/81**, 1210 (1993).
12. S.J. Zinkle, Nucl. Instr. Meth. B **91**, 234 (1994).
13. S.J. Zinkle, J. Nucl. Mater. **219** (1995) in press.
14. J.F. Ziegler, J.P. Biersak and U.L. Littmark, *The Stopping and Range of Ions in Solids* (Pergamon Press, New York, 1985).
15. P. Agnew, Phil. Mag. A **65**, 355 (1992).
16. S.J. Zinkle et al., J. Eln. Microsc. Tech. **19**, 452 (1991).
17. R.E. Stoller and G.R. Odette, J. Nucl. Mater. **141-143**, 647 (1986).
18. S.J. Zinkle and S. Kojima, J. Nucl. Mater. **179-181**, 395 (1991).
19. K.P.D. Lagerlof, T.E. Mitchell and A.H. Heuer, J. Am. Cer. Soc. **72**, 2159 (1989).
20. S.J. Zinkle, in *15th Int. Symp. on Effects of Radiation on Materials, ASTM STP 1125*, edited by R.E. Stoller et al. (Amer. Soc. Testing Mater., Philadelphia, 1992), pp. 749-763
21. R. Sizmann, J. Nucl. Mater. **69&70**, 386 (1968).
22. J.W. Corbett and J.C. Bourgoin, IEEE Trans. Nucl. Sci. **NS-18** (6), 11 (1971).
23. J.C. Bourgoin and J.W. Corbett, Phys. Lett. **38A**, 135 (1972)
24. J.C. Bourgoin and J.W. Corbett, Rad. Eff. **36**, 157 (1978).
25. S. Clement and E.R. Hodgson, Phys. Rev. B **36**, 3359 (1987).
26. Y. Chen, M.M. Abraham and H.T. Tohver, Phys. Rev. Lett. **37**, 1757 (1976).
27. Y. Chen, R. Gonzalez and K.L. Tsang, Phys. Rev. Lett. **53**, 1077 (1984).
28. M.L. Dalal, M. Rahmani and P.D. Townsend, Nucl. Instr. Meth. B **32**, 61 (1988).
29. J. Valbis and N. Itoh, Rad. Eff. Def. Solids **116**, 171 (1991).
30. E.A. Kotomin, A.I. Popov and A. Stashins, J. Phys. Condensed Mat., **6** (38), L569 (1994).
31. L.W. Hobbs, F.W. Clinard Jr., R.C. Ewing and S.J. Zinkle, J. Nucl. Mat. **216**, 291 (1994).

S.J. Zinkle 9 6

DISCLAIMER

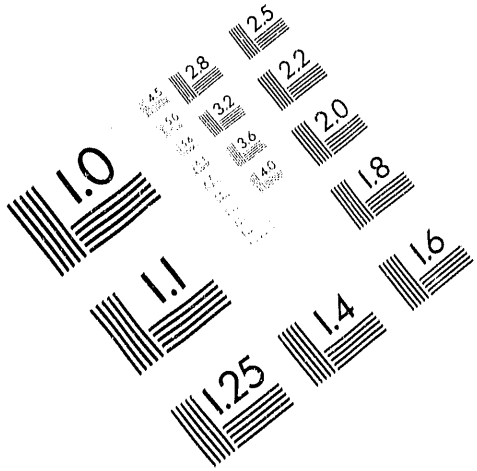

Association for Information and Image Management
1100 Wayne Avenue, Suite 1100
Silver Spring, Maryland 20910
301/587-8202

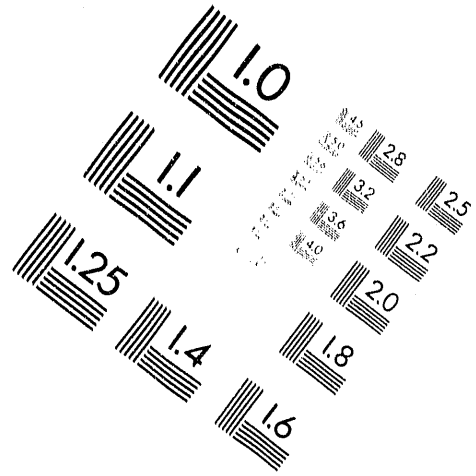

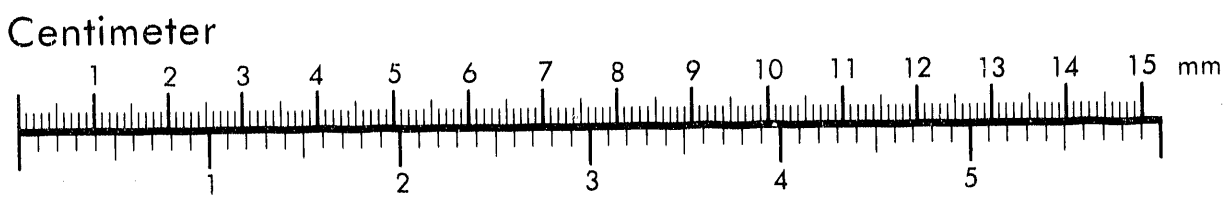

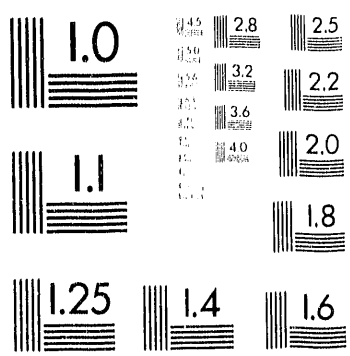

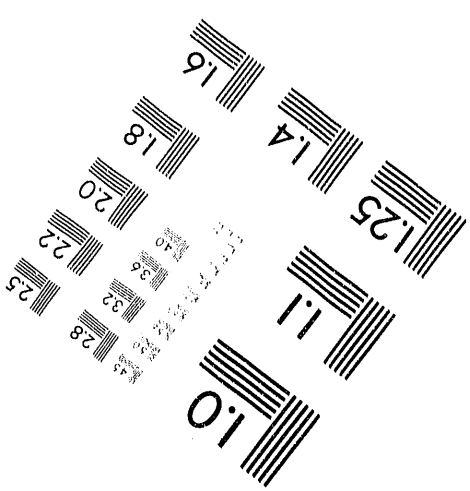

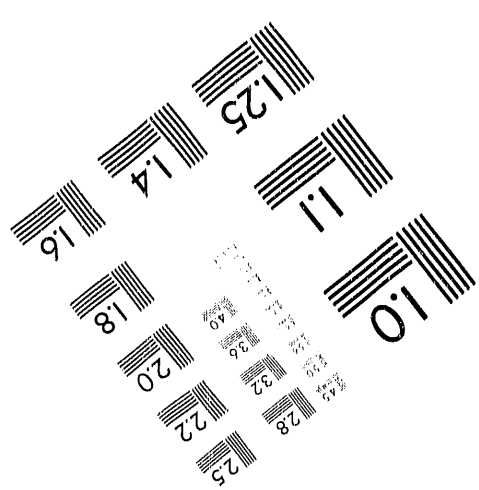

MANUFACTURED TO AIIM STANDARDS
BY APPLIED IMAGE, INC.

DATE FILMED

6/21/95

END